



## Hypersonic aerodynamics of a flat plate: Bridging formula and wall temperature effects

Yuan Hu, Song Chen, and Quanhua Sun

Citation: [AIP Conference Proceedings](#) **1501**, 1493 (2012); doi: 10.1063/1.4769715

View online: <http://dx.doi.org/10.1063/1.4769715>

View Table of Contents: <http://scitation.aip.org/content/aip/proceeding/aipcp/1501?ver=pdfcov>

Published by the [AIP Publishing](#)

---

### Articles you may be interested in

[Study of the coupling between real gas effects and rarefied effects on hypersonic aerodynamics](#)

AIP Conf. Proc. **1501**, 1515 (2012); 10.1063/1.4769718

[Comparative study of various approaches for modeling transitional hypersonic rarefied gas flows over blunt bodies](#)

AIP Conf. Proc. **1501**, 1500 (2012); 10.1063/1.4769716

[Coupling particle simulation with aerodynamic measurement in hypersonic rarefied wind tunnel in JAXA](#)

AIP Conf. Proc. **1501**, 1213 (2012); 10.1063/1.4769680

[Effects of continuum breakdown on hypersonic aerothermodynamics for reacting flow](#)

Phys. Fluids **23**, 027101 (2011); 10.1063/1.3541816

[Aerodynamics of Two Interfering SimpleShape Bodies in Hypersonic RarefiedGas Flows](#)

AIP Conf. Proc. **663**, 489 (2003); 10.1063/1.1581586

---

# Hypersonic Aerodynamics of a Flat Plate: Bridging Formula and Wall Temperature Effects

Yuan Hu, Song Chen, and Quanhua Sun<sup>a</sup>

*State Key Laboratory of High Temperature Gas Dynamics  
Institute of Mechanics, Chinese Academy of Sciences, Beijing 100190, China  
<sup>a</sup>Email: qsun@imech.ac.cn*

**Abstract.** Hypersonic flow over a flat plate is investigated under a wide range of Mach and Knudsen numbers using both continuum-based approach and DSMC method. The simulated gas is argon thus to isolate the high temperature effects. The Mach number of the flow lies between 5 and 30 whereas the Knudsen number covers the entire flow regime. It is learned that local rarefaction is observed near the leading edge even when the Knudsen number is around 0.001. The continuum breakdown can be identified using a nonequilibrium parameter that evaluates the difference among the temperature components. It is also learned that there is competition between viscous effects and rarefied effects on the skin friction. The total drag on the plate can be well estimated using a bridging formula that connects the results from the continuum and free molecular expressions. In addition, the value of drag depends on the surface temperature. The drag coefficient increases with the surface temperature when the Knudsen number is less than 0.01 but decreases when the Knudsen number is larger than 1.0.

**Keywords:** Hypersonic flow, Flat plate, Bridging formula, DSMC method.

**PACS:** 47.40.Ki, 47.45.-n

## INTRODUCTION

There are increasingly interests in hypersonic flight in the near space. Many studies have been done on aircraft configuration with high ratio of lift to drag. However, the performance of an aircraft depends strongly on the flight altitude. In addition, flat plate configuration is a limit case with good ratio of lift to drag. It is beneficial to study the aerodynamics of a flat plate under a wide range of Mach number and Knudsen number.

The flat plate geometry is very simple whereas the flow physics is quite complex. When hypersonic flow passes the plate, the flow speed will decrease and a thick boundary layer will be generated. Thus part of the gas will move outward and generates a bow shock in front of the plate. This shock wave will interact with the boundary layer where both the viscous effect and rarefied gas effect will contribute on the flow patterns.

In the literature, the hypersonic flow over the plate has been numerically investigated using continuum-based approach and kinetic based approach. In the frame of continuum theory, the flow can be divided into several zones using a viscous interaction concept. In the strong viscous interaction zone, velocity slip and temperature jump has been introduced [1]. Thus kinetic based approach is more appropriate to study this kind of flow. BGK based approach and direct simulation Monte Carlo (DSMC) method have been applied. For instance, Aoki etc. studied the problem when the Mach number lies between 1.5 and 8 by solving the BGK equation [2]. Bird investigated the aerodynamics when the Knudsen number varies from 0.1 to 10 [3]. The range of Mach and Knudsen numbers studied, however, was very limited.

In this paper, we aim to cover a wide range of Mach and Knudsen numbers for hypersonic flow over a flat plate. In order to isolate high temperature effects, monatomic gas argon is considered. This study compares the difference between continuum based and kinetic based simulation results, whose approaches are introduced in the next section followed by flow field illustration and drag analysis. In the end, the effect of wall temperature is investigated.

## NUMERICAL APPROACHES

It is aimed to investigate the hypersonic aerodynamics of a flat plate over a wide range of Mach ( $Ma$ ) and Knudsen ( $Kn$ ) numbers in this study. The Mach number ranges from 5 to 25 and the Knudsen number varies from  $10^{-5}$  to 10. Namely, the flow regimes cover the continuum and the rarefied (slip, transitional and free molecular)

flows. In terms of physical accuracy and numerical efficiency, a continuum-based CFD approach and the kinetic based direct simulation Monte Carlo (DSMC) method are employed.

The continuum-based CFD approach solves the Navier-Stokes (NS) equations using the finite volume method. To get second order accuracy, the monotone upstream schemes of conservation laws (MUSCL) with the min-mod limiter is adopted for space discretization. The convective flux and viscous terms are solved using the Roe's flux difference splitting (FDS) and center-difference schemes, respectively. These schemes are packaged in our in-house CFD code SPACER that has been extensively used to simulate hypersonic flows [4]. It is learned that the hypersonic aerodynamics is very sensitive to the numerical mesh [5], and mesh independent results are obtained through strict mesh independent study. For the accepted meshes, the surface grid Reynolds number is less than 5 and the coarsening ratio between neighboring levels is less than 1.1.

The standard DSMC method [6] is implemented in our in-house code SUPGAS. For this study, the variable hard sphere (VHS) model is employed. In principle, the DSMC method can be applied to the continuum flow. However, the requirements of DSMC on time step and cell size make the computational cost approximately proportional to  $Kn^{-3}$  for two-dimensional problems and to  $Kn^{-4}$  for three-dimensional problems, leading to the application of standard DSMC to continuum flow practically impossible. In our simulation, the cell size or the size of sub-cell is less than one third of the local mean free path of gas molecules.

In this paper, we apply the DSMC method to simulate the flows for  $Kn$  as low as  $2.5 \times 10^{-4}$  and apply the CFD approach for  $Kn$  up to 0.125. Here all the DSMC simulations are regarded physically accurate whereas the CFD results are valid only for small  $Kn$  flows. The CFD results for larger  $Kn$  flows are provided merely for establishment of a bridge function over the entire flow regime.

## FLOW FIELD ANALYSIS

The flat plate geometry is very simple, whereas the flow patterns with the plate are quite complex. Along the plate starting from the leading edge, the flow experiences free-molecular, transitional, slip or even continuum flow regimes. Therefore, difference can be observed between CFD and DSMC results even for small  $Kn$  number flows. Figure 1 compares the pressure contours at several Knudsen numbers when  $Ma=10$ . When the flow is near-continuum ( $Kn=1.25 \times 10^{-3}$ ), the shock structure is clearly seen in the flow field. The CFD result generally agrees well with the DSMC result except differences at the leading edge of the flat plate. As  $Kn$  increases to 0.0125, the shock becomes thick and the size of the disturbed area increases. The departure of the CFD result from the DSMC result becomes larger. For instance, the DSMC method predicts a larger disturbed area and smaller surface pressure. As it enters the transitional flow regime ( $Kn=0.125$ ), the CFD method fails completely.

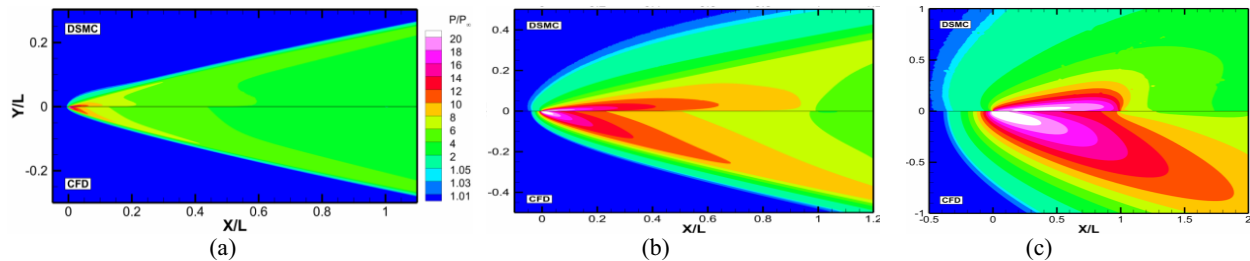


**FIGURE 1.** Comparison of pressure contours obtained from DSMC and CFD simulations at different  $Kn$  number when  $Ma=10$ . (a)  $Kn=1.25 \times 10^{-3}$ , (b)  $Kn=0.0125$ , (c)  $Kn=0.125$ .

It has been observed in Fig. 1 that there are obvious differences between the CFD and DSMC results, which means that continuum breakdown may happen locally even when the Knudsen number is as low as  $1.25 \times 10^{-3}$ . There are a lot of continuum breakdown parameters in literatures, including Bird's  $P$  parameter ( $P_{Bird}$ ) [7], the gradient length local Knudsen number ( $Kn_{GLL}$ ) [8], and non-dimensional entropy generation rate ( $Kn_S$ ) [9]. Their definitions are as follows,

$$P_{Bird} = \frac{U}{\rho v} \left| \frac{d\rho}{ds} \right|, \quad (1)$$

$$Kn_{GLL,Q} = \frac{\lambda}{Q} \left| \frac{dQ}{dl} \right|, \quad (2)$$

$$Kn_{GLL,MAX} = \max(Kn_{GLL,D}, Kn_{GLL,T}, Kn_{GLL,V}), \quad (3)$$

$$Kn_S = \frac{\lambda \dot{S}_{gen}}{\rho R \sqrt{RT}}, \quad (4)$$

$$\dot{S}_{gen} = \frac{\Phi}{T} + \frac{\kappa}{T^2} (\nabla T \cdot \nabla T). \quad (5)$$

Here,  $|d\rho/ds|$  in Eq.(1) indicates the gradient of density in the direction of streamline. The subscript D, T, V in Eq. (3) represents density, temperature, and velocity, respectively.  $\Phi$  is the dissipation function, and  $\kappa$  is the thermal conductivity. It is assumed that continuum breakdown occurs when  $P_{Bird} > 0.05$  or  $Kn_{GLL,MAX} > 0.05$ , or  $Kn_S > 0.1$ , which corresponds to a significant deviation from equilibrium.

In fact, continuum breakdown means that the non-equilibrium of a flow becomes non-negligible. One feature of strong non-equilibrium for atomic gases is that the components of translational temperature at different directions are different. Based on this fact, we can propose a post-verification continuum breakdown parameter, namely,

$$NE_T = \max \left( \left| \frac{T_x - T}{T} \right|, \left| \frac{T_y - T}{T} \right|, \left| \frac{T_z - T}{T} \right| \right), \quad (6)$$

where,  $T$  is the average translational temperature. The distribution of  $NE_T$  in the flow field of  $Ma=10$  and  $Kn=1.25 \times 10^{-3}$  is shown in Fig. 2(a). It can be seen that the shock wave and boundary layer can be clearly identified using this parameter. The region when  $NE_T \geq 0.3$  approximately corresponds to where the CFD and DSMC results exhibit significant differences at the leading edge of the flat plate. We also present the distributions for other continuum breakdown parameters in Fig. 2. The comparison shows that the non-dimensional entropy generation rate ( $Kn_S$ ) has a relatively good performance for this case.  $P_{Bird}$  predicts a much high value in the shock region whereas  $Kn_{GLL}$  overestimates the extend of non-continuum region around the surface.

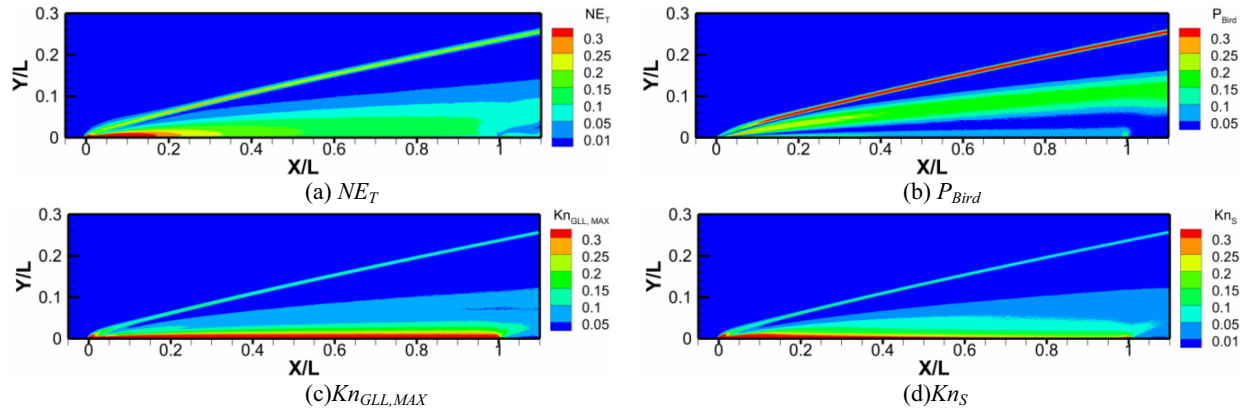


**FIGURE 2.** Comparison of contours of continuum breakdown parameters based on the DSMC results when  $Ma=10$  and  $Kn=1.25 \times 10^{-3}$ .

## DRAG ON THE FLAT PLATE

For hypersonic flows, many facts play role on the flow field, which is quite difficult to describe clearly all the features. The drag, however, is a very important aerodynamic feature. It is only a number so it is very easy to compare. Thus, we investigate the drag behavior of the flow over the flat plate.

### Skin Friction Distributions

Figure 3 shows the distributions of the skin friction coefficient predicted using the CFD and DSMC methods at several Knudsen numbers when  $Ma=10$ . The skin friction coefficient is defined as

$$C_f = \frac{\tau_w}{\rho_\infty U_\infty^2 / 2}, \quad (7)$$

where  $\tau_w$  is the shear stress on the wall,  $\rho_\infty$  and  $U_\infty$  are the free stream density and velocity, respectively. When  $Kn=1.25 \times 10^{-3}$ , the CFD profiles are generally in good agreements with the DSMC results. The difference is observed at the beginning of the flat plate where the local non-equilibrium effects are significant. In this region, the DSMC results vary non-monotonically, and are smaller than their CFD counterparts.

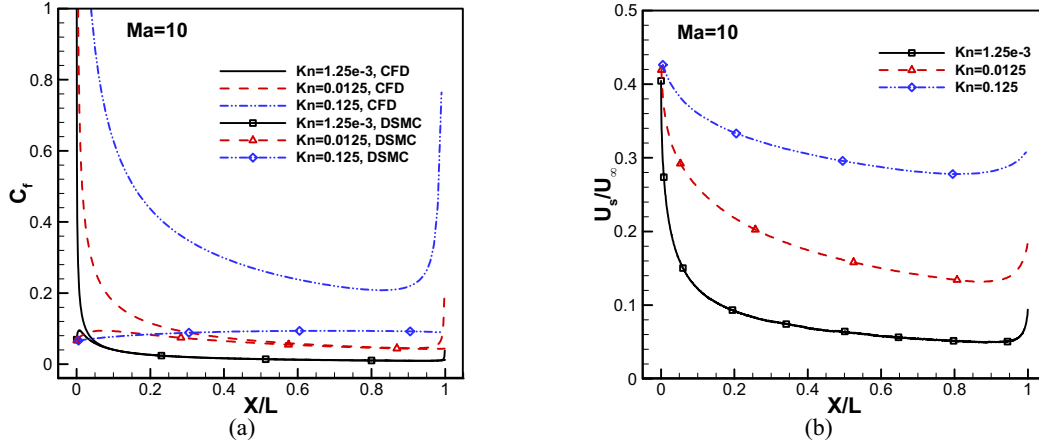


**FIGURE 3.** Comparison of skin friction coefficients and slip velocity distributions at different  $Kn$  number when  $Ma=10$ . (a) skin friction coefficient, (b) slip velocity

The skin friction reduction in the non-equilibrium region is due to the slip-flow effects. The shear stress on the wall can be expressed as  $\tau_w = \mu_w (\partial u / \partial n)_w$ . The slip velocity will reduce the normal gradient of the tangential velocity next to the wall, and thus reduces the skin friction. It is shown in Fig. 3(b) that there is considerable velocity slip (nondimensionalized by the free stream velocity) on the wall near the leading edge even when the Knudsen number is  $1.25 \times 10^{-3}$ .

For a fixed Mach number, we can see that skin friction coefficients predicted using CFD increase considerably as the Knudsen number increases. In fact, the Reynolds ( $Re$ ) number decreases as the Knudsen number increases when the Mach number is fixed since  $Re \propto Ma / Kn$ . The decrease of the Reynolds number means that the viscous effects of the flow enhance. Thus, the skin friction coefficient will increase. On the other hand, the increase of the Knudsen number causes larger slip velocity, which leads to a decrease of the skin friction coefficient. This is verified by the DSMC results that the skin friction coefficient predicted by DSMC is much less than the CFD results at the same  $Kn$  number. In summary, the increase of Knudsen number will cause the enhancement of both viscous and rarefied effects. The former will increase the skin friction coefficient whereas the later decreases it, which leads to a competition between the two effects on the contribution to the skin friction coefficient regarding the Knudsen number variation.

### Bridging Formula for Drag Coefficients

It is desired to have a simple form to estimate the drag on the plate for engineering design. The drag coefficient can be obtained by integrating the skin friction coefficient over the flat plate:

$$C_D = \frac{1}{L} \int_0^L (C_{f,upper} + C_{f,lower}) dx. \quad (8)$$

The subscripts 'upper' and 'lower' in Eq.(8) indicate the two sides of the plate.

The bridging formulas are widely used to compute the aerodynamic forces over the whole flow regimes. Fan et.al. [10] has proposed a bridging formula which predicted accurately the drag coefficient of the flat plate for low speed rarefied flow. This bridging formula has a very concise form,

$$C_D = \frac{C_{D,C} \times C_{D,FM}}{C_{D,C} + C_{D,FM}}. \quad (9)$$

The subscripts  $C$  and  $FM$  in Eq.(9) represent the expressions of drag coefficients under the continuum and the free molecular condition, respectively. A reason why Eq.(9) has been successful for low speed flow is that the theoretical solutions for drag coefficients of both continuum and free molecular flow can be easily obtained. Although the solution for high speed free molecular flow is the same as that for low speed flow, there is no analytic solution for the drag coefficient of high speed continuum flow.

In order to get the expression of  $C_{D,C}$  for high speed flows, we fit the drag coefficients obtained by our CFD simulations. A key step to succeed in getting the fitting formula of  $C_{D,C}$  for high speed flow is the appropriate choice of the correlation parameter. The so-called wall Knudsen number  $Kn_w$  proposed by Woronowicz and Baganoff [11]

has been selected. It can be seen from Fig. 4(a) that by using  $Kn_w$ , the drag coefficients approximately collapse to a single line. Thus, we can write down the expression of the fitting formula as,

$$\ln(C_{D,c} \cdot Ma) = 1.361 + 0.628 \ln(Kn_w). \quad (10)$$

The drag coefficient of free molecular flow over a flat plate is

$$C_{D,FM} = \sqrt{\frac{8}{\pi\gamma}} \frac{1}{Ma}, \quad (11)$$

where  $\gamma$  is the ratio of specific heats, which is 5/3 for argon. However, when applying equations (10) and (11) in Eq. (9), the bridging formula does not capture the non-monotonic variation of the drag coefficients in the transitional regime. We then add a modification term to Eq. (9) so that its validity can be extended to the transitional regime. The modified form of  $C_{D,FM}$  in Eq. (9) is written as  $C_{D,FM,E}$ ,

$$C_{D,FM,E} = \sqrt{\frac{8}{\pi\gamma}} \frac{1}{Ma} (1 + 0.1\sqrt{Re}). \quad (12)$$

It is shown in Fig. 4(b) that the results predicted by the bridging formula agree fairly well with the numerical results in a wide range of Mach number over the whole flow regimes.

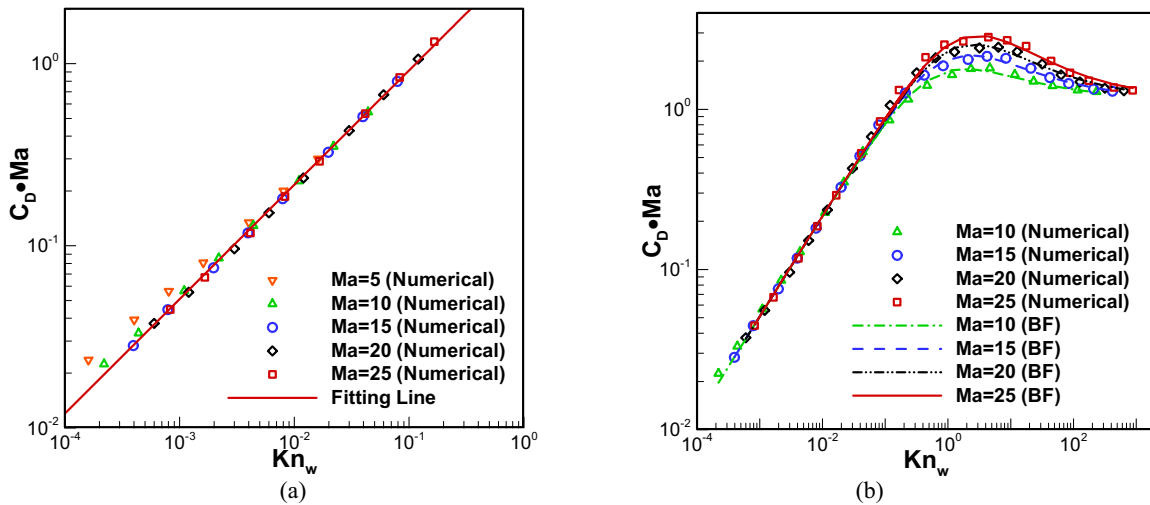


FIGURE 4. Drag on the flat plate for hypersonic flows. (a) continuum results, (b) bridging function.

## WALL TEMPERATURE EFFECTS ON AERODYNAMICS

The temperature variation on the surface can affect the aerodynamics of vehicles. However, the aero-thermal environment around a hypersonic vehicle is very complicated. The wall temperature cannot be exactly known in advance. Therefore, we investigate the aerodynamics at several typical wall temperatures so as to provide useful information for practical applications.

Figure 5 shows the influence of wall temperature on the skin friction distributions at several Knudsen numbers when  $Ma=10$ . The wall temperatures are set as 200K, 500K, 1000K and 2000K, respectively. When the flow is near-continuum ( $Kn=1.25 \times 10^{-3}$ ), the skin friction coefficient increases as the surface temperature increases, except for the immediate neighborhood of the leading edge. The increase of skin friction with surface temperature is caused by the fact that the viscosity is proportional to the temperature ( $\mu \propto T^\omega$ ) and the rarefied gas effects are not significant. As  $Kn$  increases to 0.125, the influence of rarefied gas effects become important and the change of skin friction coefficient with the increasing wall temperature is complex. In the region of  $x/L < 0.4$ , the skin friction coefficient decreases as the surface temperature increases. This is because the rarefied gas effects or the slip effects, which cause a decrease of skin friction coefficient, become dominant in this region when it is the transitional flow, and the increasing wall temperature enhances the slip effects as shown in Fig. 6. As approaching to the end of the plate, the rarefied gas effects are gradually weakened. Thus, it can be seen that higher wall temperature corresponds to higher skin friction coefficient at the end of the plate, where the viscous effects become dominant again. However, as  $Kn$  increases to 1.25, the influence of rarefied gas effects is dominant around the surface of the entire flat plate, so no region where higher surface temperature corresponds to higher skin friction coefficient is observed in our simulation.

Figure 7 shows influence of surface temperature on total drag coefficient. The drag coefficient changes non-monotonically with not only increasing the Knudsen number but also the surface temperature. As the surface temperature increases, the viscous effects are significant at low Knudsen numbers, while the rarefied gas effects are dominant at high Knudsen numbers. When  $Kn$  is less than about 0.01, the total drag coefficient increases with the increase of surface temperature at all Mach numbers; and when  $Kn$  is larger than about 1.0, the total drag coefficient decreases as the surface temperature increases until the free molecular limit is reached. The corresponding Knudsen number at which the trend of total drag coefficient variation with surface temperature turns depends on the Mach number. In particular, it can be observed that when  $Ma=10$  and  $Kn=0.125$ , the total drag coefficient first increases as the surface temperature increases from 200K to 500K; as the surface temperature continues increasing, the total drag coefficient, however, keeps decreasing.

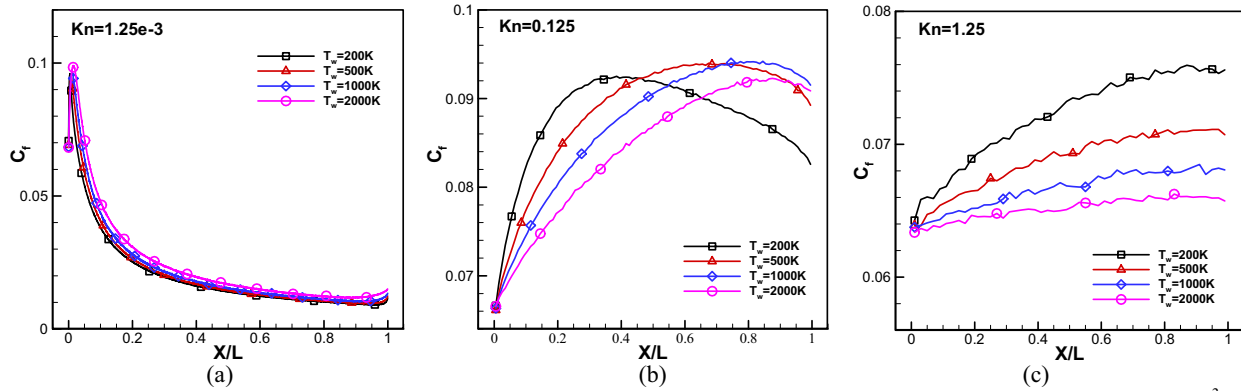


FIGURE 5. Skin friction coefficient at different Knudsen numbers and surface temperatures when  $Ma=10$ . (a)  $Kn=1.25 \times 10^{-3}$ , (b)  $Kn=0.125$ , (c)  $Kn=1.25$ .

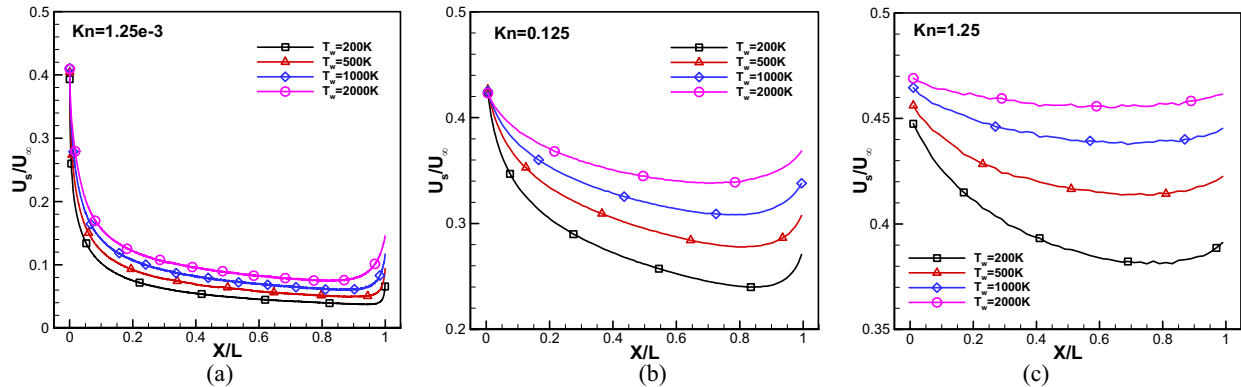


FIGURE 6. Slip velocity at different Knudsen numbers and surface temperatures when  $Ma=10$ . (a)  $Kn=1.25 \times 10^{-3}$ , (b)  $Kn=0.125$ , (c)  $Kn=1.25$ .

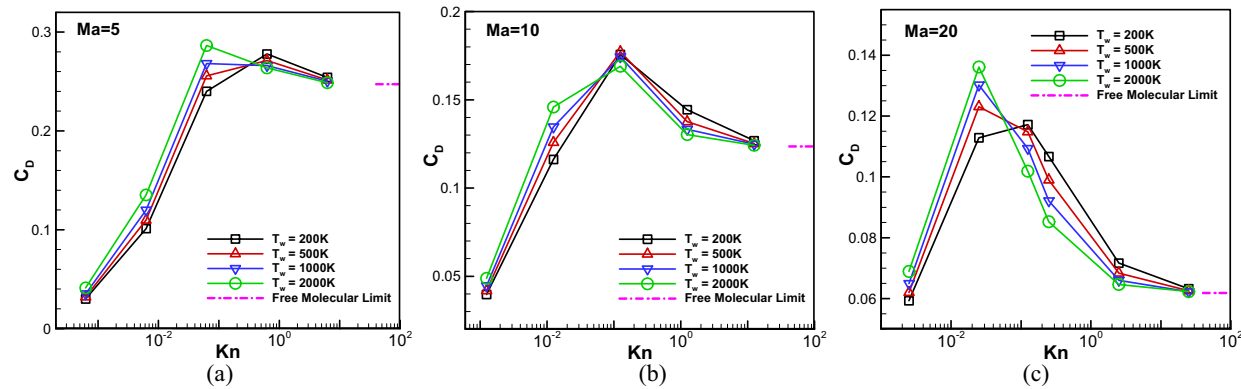


FIGURE 7. Influence of surface temperature on the drag coefficient at different Mach and Knudsen numbers. (a)  $Ma=5$ , (b)  $Ma=10$ , (c)  $Ma=20$ .

## CONCLUDING REMARKS

The supersonic flow over a flat plate is investigated using both the continuum-based approach and the DSMC method. After having the numerical results that cover a large range of Mach and Knudsen numbers, we can draw some conclusions.

First, the flow involves shock wave and boundary layer. Rarefaction is observed near the leading edge even when the  $Kn$  number is around 0.001, thus the continuum based approach fails to capture the flow detail. The continuum breakdown can be identified using a nonequilibrium parameter  $NE_T$  that evaluates the difference among the temperature components. It is safe to say that the continuum assumption is invalid when this parameter is larger than 0.3.

Second, there is competition between viscous effects and rarefied effects on the skin friction. The increase of Knudsen number will cause the enhancement of both viscous and rarefied effects. The former will increase the skin friction coefficient whereas the later decreases it. The total drag on the plate can be well estimated using a bridging formula that connects the results from the continuum and free molecular expressions.

Third, the drag depends on the surface temperature. The drag coefficient increases with the surface temperature when  $Kn$  is less than 0.01 and decreases when  $Kn$  is larger than 1.0. However, it should be mentioned that the current study concerns only the monatomic gas argon, thus the high temperature effects are not included.

## ACKNOWLEDGMENTS

The authors would like to acknowledge the support from the National Natural Science Foundation of China with grants 10742001 and 90816012.

## REFERENCES

1. H. Oguchi, "Leading Edge Slip in Rarefied Hypersonic Flow" in *Rarefied Gas Dynamics*, vol. 2, edited by J. A. Laurmann, Academic Press Inc., New York, 1963, pp. 181-193.
2. K. Aoki, K. Kanba, and S. Takata, *Phys. Fluids* **9**, 1144-1161 (1997).
3. G. A. Bird, *AIAA J.* **4**, 55-60 (1966).
4. H. Zhu, G. Wang, Q. Sun, and J. Fan, *Acta Aerodyn Sin.*, (in press) (2012).
5. Q. Sun, H. Zhu, G. Wang, and J. Fan, *Theor. Appl. Mech. Lett.* **1**, 022001 (2011).
6. G. A. Bird, *Molecular Gas Dynamics and the Direct Simulation of Gas Flows*, Oxford: Clarendon Press, 1994.
7. G. A. Bird, *AIAA J.* **8**, 1998-2003 (1970).
8. W. L. Wang, and I. D. Boyd, *Phys. Fluids* **15**, 91-100 (2003).
9. P. H. Chen, I. D. Boyd, and J. Camberos, AIAA Paper 2003-3783 (2003).
10. J. Fan, C. Wu, Q. Sun, and J. Jiang, *Adv. Mech.* (in Chinese) **39**, 421-425 (2009).
11. M. Woronowicz, and D. Baganoff, *J. Thermophys. Heat Transf.* **7**, 63-67 (1993).